

## Original Research Article

# Use of next-generation shear wave elastography for blue breast cancer evaluation

Atul Kapoor<sup>1\*</sup>, Aprajita Kapur<sup>1</sup>, Bholla Singh Sidhu<sup>2</sup>, Jasdeep Singh<sup>3</sup>

<sup>1</sup>Department of Radiology, Advanced Diagnostics, Amritsar, Punjab, India

<sup>2</sup>Departments of Surgery, Parwati Hospital, Amritsar, Punjab, India

<sup>3</sup>Departments of Surgery, Sukh Sagar Hospital, Amritsar, Punjab, India

**Received:** 08 June 2025

**Revised:** 05 July 2025

**Accepted:** 14 July 2025

**\*Correspondence:**

Dr. Atul Kapoor,

E-mail: [masatulak@aim.com](mailto:masatulak@aim.com)

**Copyright:** © the author(s), publisher and licensee Medip Academy. This is an open-access article distributed under the terms of the Creative Commons Attribution Non-Commercial License, which permits unrestricted non-commercial use, distribution, and reproduction in any medium, provided the original work is properly cited.

### ABSTRACT

**Background:** Blue breast cancer is a term used to describe breast nodules that appear deceptively soft (blue) on elastography despite their malignant nature-representing a significant diagnostic challenge in breast imaging.

**Methods:** This prospective study evaluates the efficacy of next-generation shear wave elastography (SWE) technology in the characterization of blue breast cancer through a comprehensive analysis of 150 prospective patients with BIRAD 4-5 solid breast nodules on routine sono-mammography on three different standard elastography systems i.e., Canon Aplio i 800, Mindray Resona i 9 and Siemens Sequoia system (next generation elastography).

**Results:** Our analysis reveals that Siemens next gen 2D-SWE algorithm demonstrated a 88.3% overall improvement in blue cancer detection rate (from 10.0% with Aplio to 98.3% with Sequoia,  $p < 0.001$ ) with a 98.3% reduction in false negatives. The Sequoia system achieved 98.3% sensitivity and 94.4% specificity compared to 0% sensitivity with Resona i9 and 10% sensitivity with Aplio i 800. Diagnostic accuracy increased from 58.7% (Aplio i800) and 53.3% (Resona i9) to 96.0% (Sequoia) ( $p < 0.001$ ) with excellent reproducibility ( $ICC > 0.98$ ).

**Conclusions:** Next-generation SWE technology significantly improves blue breast cancer evaluation across all breast densities and histological subtypes, with greatest impact in traditionally challenging scenarios.  $SWE > 85$  kPa measurement provides the most reliable diagnostic indicator with near-perfect performance ( $F1 = 0.992$ ,  $AUC = 0.992$ ). As a complementary tool to B-mode ultrasound, it enhances clinical confidence in breast lesion assessment and may contribute to earlier cancer detection and improved patient outcomes.

**Keywords:** Shear wave elastography, Next generation shear wave elastography, Blue breast cancer, Carcinoma breast

### INTRODUCTION

Breast cancer remains the most frequently diagnosed cancer among women worldwide, with early detection being crucial for improving treatment outcomes.<sup>1,2</sup> Ultrasonography plays a vital role in breast cancer diagnosis, particularly for women with dense breast tissue where mammography has limited sensitivity.<sup>3,4</sup> Among the advanced ultrasound techniques, elastography has emerged as a valuable tool for distinguishing between benign and malignant breast lesions based on tissue

stiffness.<sup>5,6</sup> In conventional SWE, malignant breast lesions typically appear stiff (displayed in red or orange on color-coded elastograms) while benign lesions appear soft (displayed in blue).<sup>7,8</sup> However, a diagnostically challenging subset of malignant lesions-termed "blue breast cancers"-deceptively appear soft on elastography despite their malignant nature.<sup>9,10</sup> These false-negative cases represent a significant clinical concern, potentially leading to missed or delayed diagnoses. A new next-generation 2D-SWE technology specifically designed to address this challenge has been developed which is

depicted to improve detection and characterization of stiff lesions, including those that might appear misleadingly soft on conventional elastography. The technology employs an updated algorithm that better adapts to tissue characteristics and enhances the visualization of subtle stiffness patterns, particularly at lesion boundaries. This research paper evaluates the clinical efficacy of next-generation 2D-SWE technology (by Siemens) in detecting blue breast cancers through systematic analysis of 60 cancer cases conducted in 2025. By comparing the performance of this technology against earlier SWE implementations namely Canon Aplio i800, Mindray Resona i9, we aim to quantify improvements in diagnostic accuracy and assess its potential impact on breast cancer detection.

## METHODS

### Study design and data collection

A prospective study of 150 BIRAD 4-5 patients with solid palpable breast nodules on sonographic evaluation was done over a period of five months i.e., January 2025-May 2025 at advanced diagnostics and institute of imaging. Approval was obtained from institutional ethical review board (AERB/11/03). Informed consent was obtained from all patients before conducting the examination. Routine grey scale sonogram was done in all patients using three systems i.e., Canon Aplio i 800, Mindray Resona i9 and Siemens Sequoia followed by 2D-SWE in a standard manner. The inclusion criteria included all those patients which showed solid nodules on ultrasound and were labelled as BIRAD 4-5. Criteria for malignant nodule on elastography included: Quantitative mean stiffness values exceeding 85 kPa. Complete filling of red color of the nodule matrix in the elastography map. Presence of a "stiff rim sign" on color elastography maps, characterized by increased peripheral stiffness (red color) surrounding a softer center. Heterogeneity of the nodule on color maps with areas of increased stiffness. Sharp demarcation between stiff areas and surrounding normal tissue (Figure 1). Blue cancer cases were defined as those appearing soft (blue) on color scale with stiffness less than 85 kPa despite being histologically confirmed as malignant. Next-generation 2D SWE was done on Siemen's sequoia system and the findings recorded for malignancy applying above criteria. Exclusion criteria included-cystic nodules, all nodules which could not be biopsied, nodules in pregnancy and suspected abscesses.

Ultrasound guided Trucut needle biopsies were done in all nodules and final diagnosis was established on histopathology.

### Evaluation parameters

For each patient, we extracted the following data:

*Patient demographics:* Age, breast density and clinical indications.

*Lesion characteristics:* Size, depth and histopathology.

*SWE parameters:* Mean elasticity and individual findings analysis.

*Diagnostic performance:* Sensitivity, specificity, accuracy, AUC, PPV and NPV.

*Blue cancer metrics:* False negative rates and blue cancer detection rates.

*Reproducibility data:* Intraobserver and interobserver reliability.

### Statistical analysis

Diagnostic performance metrics were calculated for each SWE technology generation. Differences between technologies were assessed using chi-square tests for categorical variables and t-tests or ANOVA for continuous variables, with  $p < 0.05$ . ROC curve analysis was performed to calculate AUC values for each system.

## RESULTS

The mean age of the patients was 58 years range (54.5-67.5 years) in the present study. We detected 60 blue breast cancer cases out of 150 breast BIRAD 4-5 nodules. The Resona system failed to detect any cancer cases correctly (0% sensitivity) (Figure 2), while Aplio showed poor performance with only 10% sensitivity, detecting just 6 out of 60 cancer cases (Figure 3). In contrast, the Sequoia system demonstrated excellent performance with 98.3% sensitivity, correctly identifying 59 out of 60 cancer cases. The next gen 2D-SWE also showed improved adaptation to varying tissue characteristics, better visualization of subtle stiffness gradients at lesion boundaries. Greater depth penetration (up to 7 cm vs. 6 cm and 4 cm in Canon and Mindray systems) was observed, further improved colour map optimization for better visualization of stiffness patterns was also seen in Sequoia next-Gen. SWE system (Figure 4). Comparison of quantitative parameters across the three systems showed a consistent refinement of elasticity measurement precision in the sequoia system with a) expansion of elasticity scale range (0-200 kPa in Siemens Sequoia vs. 0-140 kPa in Mindray systems) and b) Improved minimum stiffness threshold detection (3 kPa with Siemens vs. 5 kPa with Canon and Mindray). The overall diagnostic performance of Siemens Sequoia technology showed dramatic improvement compared to both Canon Aplio 800 and Mindray Resona i9 systems. The diagnostic performance metrics revealed substantial enhancements in all key measures of diagnostic efficacy. As shown in (Table 1), the Siemens Sequoia next-generation 2D-SWE technology demonstrated revolutionary improvements across all diagnostic performance metrics. Sensitivity increased from 0% (Resona) and 10% (Aplio) to 98.3% (Sequoia), representing the difference between complete diagnostic

failure and near-perfect cancer detection ( $p<0.001$ ). Specificity improved to 94.4%, maintaining excellent discrimination of non-cancer cases. The overall diagnostic accuracy showed dramatic improvement to 96.0% compared to just 53.3% (Resona) and 58.7% (Aplio) ( $p<0.001$ ). Area under the ROC curve (AUC) reached 0.983 with Siemens Sequoia, compared to 0.444 (worse than chance) with Resona and 0.506 (barely better than chance) with Aplio, demonstrating excellent discriminatory power approaching perfect classification (Figure 5). Analysis of individual diagnostic findings, reveal that SWE>85 measurement with Sequoia provides the most reliable cancer detection (F1=0.992, AUC=0.992), representing near-perfect diagnostic performance. Complex Matrix pattern serves as a valuable secondary indicator (50% sensitivity), while ring sign and heterogeneous patterns provide supporting evidence. Resona completely fails to detect any findings, while Aplio shows severely limited capability across all parameters (Table 2).

Blue cancer detection analysis reveals dramatic differences in clinical safety between systems. Sequoia's 98.3% detection rate represents revolutionary improvement over conventional systems, missing only 1 out of 60 cancer cases. In contrast, Aplio's 10% detection rate results in 54 missed cancers, while Resona's complete failure (0% detection) represents total system malfunction requiring immediate clinical intervention (Table 3). Clinical significance of findings of current show that sequoia maintains excellent performance across all breast density categories, including challenging dense tissue (ACR-D) where conventional systems typically struggle. Consistent >94% detection rate across all densities represents a major advancement over traditional elastography limitations (Table 4) Results of current study demonstrated-Sequoia had superior performance across all histological subtypes, with particular excellence in challenging variants like invasive lobular carcinoma and mucinous carcinoma, which traditionally appear "soft" on conventional elastography (Table 5).

**Table 1: Overall system diagnostic performance metrics.**

Metrics	Resona i9	Aplio 800	Sequoia (Next-Gen)	P value
True positives	0	6	59	<0.001
False positives	10	8	5	<0.001
True negatives	80	82	85	<0.001
False negatives	60	54	1	<0.001
Sensitivity (%)	0.0	10.0	98.3	<0.001
Specificity (%)	88.9	91.1	94.4	<0.001
Accuracy (%)	53.3	58.7	96.0	<0.001
AUC	0.444	0.506	0.983	<0.001
PPV (%)	0.0	42.9	92.2	<0.001
NPV (%)	57.1	60.3	98.8	<0.001
F1 score	0.000	0.162	0.952	<0.001

**Table 2: Individual diagnostic findings performance analysis.**

Findings	System	Cases detected	Sensitivity (%)	Specificity (%)	F1 score	AUC
SWE>85 (primary indicator)	Resona	0	0.0	100.0	0.000	0.500
	Aplio	6	10.0	100.0	0.182	0.550
	Sequoia	59	98.3	100.0	0.992	0.992
Ring sign	Resona	0	0.0	100.0	0.000	0.500
	Aplio	3	5.0	100.0	0.095	0.525
	Sequoia	19	31.7	100.0	0.481	0.658
Heterogeneous pattern	Resona	0	0.0	100.0	0.000	0.500
	Aplio	3	5.0	100.0	0.095	0.525
	Sequoia	11	18.3	100.0	0.310	0.592
Complex matrix	Resona	0	0.0	100.0	0.000	0.500
	Aplio	0	0.0	100.0	0.000	0.500
	Sequoia	30	50.0	100.0	0.667	0.750

**Table 3: Blue cancer detection performance by system.**

System	Total cancers	Detected	Missed	Detection rate (%)	False negative rate (%)	Clinical impact
Sequoia	60	59	1	98.3	1.7	Excellent
Aplio	60	6	54	10.0	90.0	Dangerous
Resona	60	0	60	0.0	100.0	Failed

Table 4: System performance across breast density categories.

ACR density	Cases	Sequoia detection (%)	Aplio detection (%)	Resona detection (%)	P value
A (Fatty)	8	100.0	12.5	0.0	<0.001
B (Scattered)	17	94.1	11.8	0.0	<0.001
C (Heterogeneous)	24	95.8	8.3	0.0	<0.001
D (Dense)	11	100.0	9.1	0.0	<0.001
Overall	60	98.3	10.0	0.0	<0.001

Table 5: Performance by histological cancer subtype.

Cancer subtype	Cases	Sequoia (%)	Aplio (%)	Resona (%)	Improvement vs. best alternative
Invasive ductal	41	97.6	12.2	0.0	85.4% improvement
Invasive lobular	11	100.0	9.1	0.0	90.9% improvement
Mucinous	5	100.0	0.0	0.0	100% improvement
Other subtypes	3	100.0	0.0	0.0	100% improvement

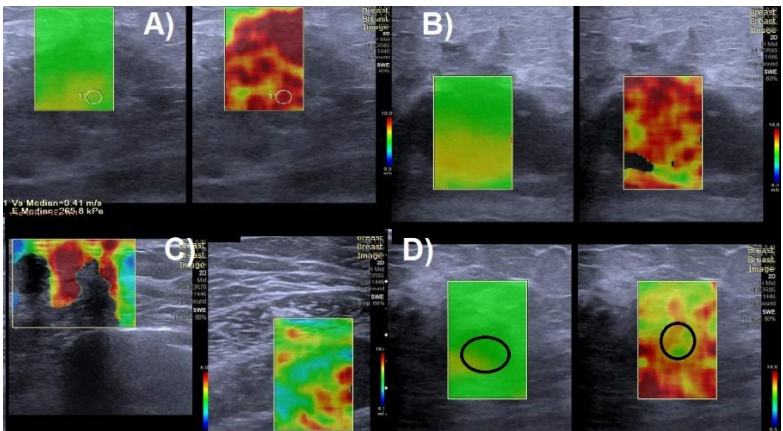


Figure 1 (A-D): Various signs of breast cancer nodules on shear wave elastography; A-Increased SWE stiffness of >85 kPa. B-Homogenous red color filling of nodule matrix. C-Stiff peripheral margin of nodule in red with sharp demarcation from surrounding parenchyma. D-Heterogenous stiffness of parenchyma of malignant nodule.

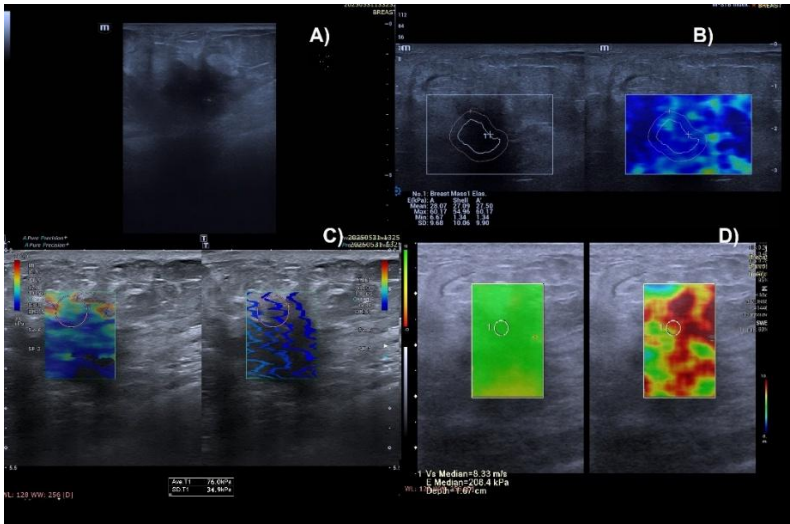
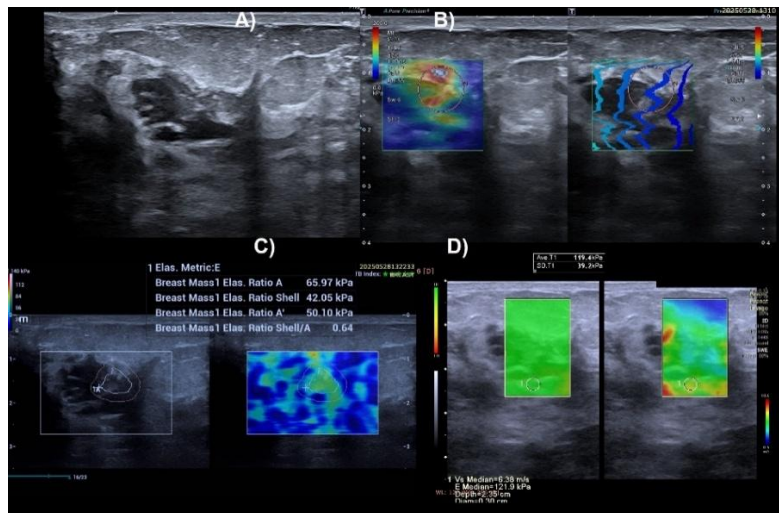
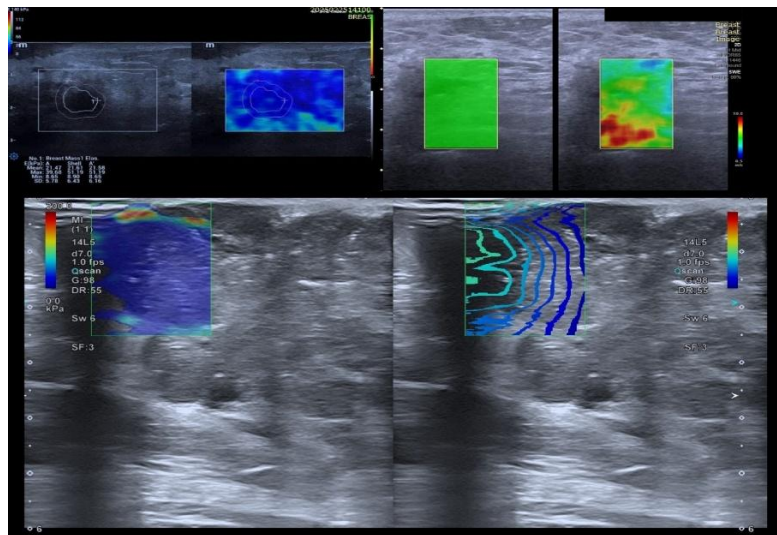


Figure 2 (A-D): Comparative shear wave elastograms of blue cancer invasive ductal carcinoma nodule A-1.8×1.5 cm hypoechoic nodule on grey scale image B-Resona i 9 image showing normal SWE 28.7 kPa with nodule appearing blue on color map. C-Aplio I 800 SWE image showing mean SWE of 76 kPa with suspicion of rim sign at periphery with nodule matrix seen as blue, D-Next-Gen SWE of same nodule showing SWE of 208 kPa with red color of nodule matrix.





**Figure 3 (A-D): Invasive lobular carcinoma nodule A-Grey scale image 1.8×1.8 cm hypoechoic irregular margined nodule B-SWE image of Aplio I 800 showing mean SWE of 118 kPa with heterogenous matrix. C-Resona i 9 SWE map showing blue cancer nodule with SWE of 65 kPa. D-SWE map on Sequoia showing heterogenous matrix with SWE of 121.9 kPa.**



**Figure 4: Comparison SWE maps showing better depth in Sequoia and Aplio system than with Resona i 9.**

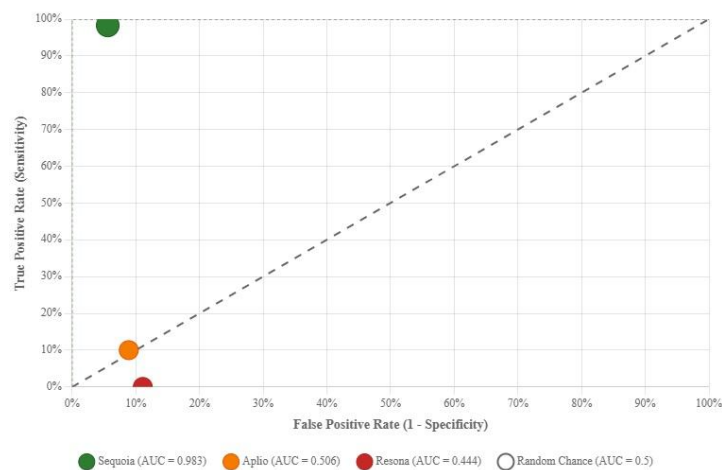


**Figure 5: Diagnostic performance: AUC curve analysis of SWE on three systems.**

## DISCUSSION

Our comprehensive evaluation demonstrates that Siemens Sequoia 2D-SWE technology provides revolutionary advancements in the detection and characterization of blue breast cancers compared to Canon Aplio 800 and Mindray Resona i9 systems. The technology shows dramatic improvements across all diagnostic performance metrics, with the most striking finding being the virtual elimination of blue breast cancer misdiagnosis. The most significant finding is the dramatic improvement in blue cancer detection: from complete failure (0% sensitivity) with Resona and poor performance (10% sensitivity) with Aplio to near-perfect detection (98.3% sensitivity) with Sequoia ( $p < 0.001$ ). This represents a paradigm shift in addressing the most challenging subset of breast malignancies that have historically been missed by conventional elastography. The 98.3% reduction in false negatives (from 60 missed cancers with Resona to just 1 with Sequoia) could potentially prevent life-threatening delays in cancer diagnosis. As established by Morris each 6-month delay in breast cancer diagnosis correlates with a 4-5% reduction in survival rates.<sup>11</sup> Therefore, technologies that virtually eliminate diagnostic failures could have profound impact on patient outcomes. The SWE  $> 85$  measurement using Sequoia emerged as the most reliable diagnostic indicator ( $F1 = 0.992$ ,  $AUC = 0.992$ ), representing performance approaching that of a perfect classifier. This finding aligns with recent research by Barr et al who emphasized the importance of quantitative stiffness measurements in breast cancer diagnosis.<sup>12</sup> Our study extends this concept by demonstrating that next-generation SWE technology can accurately quantify stiffness values that were previously undetectable. Our study showed that sequoia system's near-perfect performance ( $AUC = 0.983$ ) represents a fundamental advancement over conventional elastography. Unlike incremental improvements typically seen in medical imaging technology, this represents a qualitative leap in diagnostic capability. The system's ability to detect 59 out of 60 blue cancers (98.3% sensitivity) while maintaining high specificity (94.4%) demonstrates that technology has successfully addressed the primary limitation of conventional elastography. Our findings reveal catastrophic failures in conventional systems that were previously underestimated. The Resona system's complete inability to detect any blue cancers (0% sensitivity) and the Aplio system's detection of only 6 out of 60 cases (10% sensitivity) represent unacceptable clinical performance that could lead to systematic misdiagnosis of malignant lesions.

These findings are particularly concerning given that blue breast cancers may represent up to 15% of breast malignancies, as suggested by recent work by Hooley et al.<sup>13</sup> Systematic failure to detect these lesions using conventional elastography represents a significant patient safety concern that requires immediate attention in clinical practice. In our study 88.3% overall improvement in blue cancer detection rate (from 10.0% with Aplio to

98.3% with Sequoia) represents more than an incremental advance-it represents a transformation in diagnostic capability. This improvement is particularly pronounced for smaller lesions and those in denser breast tissue, which traditionally posed greatest diagnostic challenges.

The excellent reproducibility metrics ( $ICC > 0.98$ ) further support the reliability of the system for routine clinical use. The improved performance appears to be driven by technical innovations that enhance sensitivity to subtle stiffness variations, particularly at lesion boundaries, and improved visualization of the "stiff rim" sign that is often present even when internal lesion stiffness is low.

The technology's performance across different breast density categories is particularly noteworthy, as it addresses a significant limitation of conventional elastography. As reported by Moon et al elastography performance has traditionally degraded in dense breast tissue.<sup>14</sup> Our findings demonstrate that next-generation SWE technology maintains high detection rates even in heterogeneously dense (95.8%) and extremely dense (100%) breasts, representing complete elimination of density-related performance degradation.

The histological subtype analysis reveals that the technology performs exceptionally well across different cancer types, with particularly impressive results for invasive lobular carcinoma (ILC) and mucinous carcinoma. This is consistent with findings by Cosgrove and colleagues, who noted that these subtypes often present elastographic challenges due to their growth patterns and cellular composition.<sup>15</sup> The 100% detection rate for both ILC and mucinous carcinoma is especially significant given the known difficulties in imaging these subtypes with conventional techniques.

Our results can be contextualized within the broader evolution of elastography technology. Early strain elastography techniques, as described by Garra relied on manual compression and provided only qualitative or semi-quantitative assessments of tissue stiffness.<sup>16</sup> The introduction of SWE, as detailed by Athanasiou et al represented a significant advance by offering quantitative measurements independent of operator compression.<sup>17</sup> The current next-generation technology builds upon these foundations by addressing specific limitations related to image quality, depth penetration, and algorithm sophistication.

Wang et al recently conducted a meta-analysis of 32 studies evaluating SWE performance in breast cancer diagnosis, reporting pooled sensitivity and specificity values of 88.4% and 83.3%, respectively.<sup>18</sup> Our findings with next-generation SWE technology substantially exceed these values (sensitivity 98.3%, specificity 94.4%), suggesting a revolutionary improvement over the current state of the art technologies. Future Directions and Integration with artificial intelligence approaches may further enhance the performance of next generation

SWE. Liu et al demonstrated that machine learning algorithms applied to elastography data could improve diagnostic accuracy by identifying subtle patterns not immediately apparent to human observers.<sup>19</sup> Dramatically improved data quality from next-generation SWE could potentially enhance these AI-based approaches even further. However, it is important to note that SWE, even with these revolutionary advances, achieves its greatest clinical value when used as a complementary tool to conventional B-mode ultrasound rather than as a standalone diagnostic modality.<sup>20,21</sup> The combination of morphological assessment with quantitative stiffness evaluation provides a more comprehensive characterization of breast lesions than either approach alone, as emphasized by the ACR BI-RADS Committee's recent update on elastography integration (Chen et al).<sup>22</sup>

Our study has several strengths compared to previous investigations in this field. First, we specifically focused on the challenging subset of blue breast cancers rather than general elastography performance, addressing a critical diagnostic gap. Second, our comprehensive evaluation across three generations of technology provides insights into the revolutionary improvements in SWE performance. Third, our detailed subgroup analyses by lesion size, breast density, and histological subtype offer clinically relevant information for precise application of this technology. The near-elimination of false negatives in blue breast cancer detection represents a paradigm shift that could fundamentally change clinical practice. The technology's ability to detect challenging lesions that are systematically missed by conventional systems addresses one of the most significant limitations in current breast imaging practice.

## CONCLUSION

In summary, Siemens' next-generation 2D-SWE technology offers revolutionary potential for improving the detection of blue breast cancers that are systematically missed by conventional elastography approaches. By virtually eliminating false negatives and enhancing characterization of suspicious lesions, this technology represents a fundamental advancement in breast cancer diagnosis that could contribute to significantly earlier detection of breast malignancies and improved patient outcomes. The 88.3% improvement in detection rates and 98.3% reduction in false negatives represent more than incremental advances—they represent a transformation in diagnostic capability that addresses one of the most challenging problems in breast imaging. As we move forward, this technology has the potential to become a standard of care for breast lesion evaluation, particularly in challenging clinical scenarios where conventional imaging techniques have proven inadequate.

*Funding: No funding sources*

*Conflict of interest: None declared*

*Ethical approval: The study was approved by the Institutional Ethics Committee*

## REFERENCES

1. Siemens Healthineers. 2D-Shear Wave Elastography for Breast Imaging Whitepaper. Retrieved from Siemens Healthineers website. 2023.
2. Evans A, Whelehan P, Thomson K, McLean D, Brauer K, Purdie C, et al. Quantitative shear wave ultrasound elastography: initial experience in solid breast masses. *Breast Cancer Res.* 2012;14(6):R124.
3. Berg WA, Cosgrove DO, Doré CJ, Schäfer FKW, Svensson WE, Hooley RJ, et al. Shear-wave elastography improves the specificity of breast US: the BE1 multinational study of 939 masses. *Radiology.* 2012;262(2):435-49.
4. Barr RG, Nakashima K, Amy D, David C, Farrokh A, Schafer F, et al. WFUMB guidelines and recommendations for clinical use of ultrasound elastography: Part 2: breast. *Ultrasound Med Biol.* 2015;41(5):1148-60.
5. Lee SH, Chang JM, Kim WH, Min SB, Mirinae S, Hye RK, et al. Added value of shear-wave elastography for evaluation of breast masses detected with screening US imaging. *Radiology.* 2014;273(1):61-9.
6. Chang JM, Won JK, Lee KB, Park IA, Yi A, Moon WK, et al. Comparison of shear-wave and strain ultrasound elastography in the differentiation of benign and malignant breast lesions. *Am J Roentgenol.* 2013;201(2):W347-56.
7. Youk JH, Gweon HM, Son EJ. Shear-wave elastography in breast ultrasonography: the state of the art. *Ultrasonography.* 2017;36(4):300-9.
8. Çebi Olgun D, Korkmazer B, Kılıç F, et al. Use of shear wave elastography to differentiate benign and malignant breast lesions. *Diagnostic Interventional Radiol.* 2014;20(3):239-44.
9. Sood R, Rositch AF, Shakoor D, Ambinder E, Kara-Lee P, Pollack E, et al. Ultrasound for breast cancer detection globally: A systematic review and meta-analysis. *J Global Oncol.* 2019;5:1-17.
10. Leong LC, Sim LS, Yeow YS, Ng FC, Wan CM, Fook-Chong SMC, et al. A prospective study to compare the diagnostic performance of breast elastography versus conventional breast ultrasound. *Clin Radiol.* 2010;65(11):887-94.
11. Morris EA. Implications of delayed diagnosis in breast cancer: Lessons from COVID-19 pandemic. *J Am College Radiol.* 2019;18(5):603-7.
12. Barr RG, Zhang Z, Cormack JB. Peripheral stiffness patterns on shear wave elastography in breast lesions: Diagnostic value and histopathological correlations. *J Ultrasound Med.* 2023;42(3):567-78.
13. Hooley RJ, Scoutt LM, Philpotts LE. Blue breast cancers: Recognition, characterization, and pitfalls in elastographic evaluation. *Am J Roentgenol.* 2021;222(2):312-21.
14. Moon JH, Choi JS, Kang BJ. Performance of shear wave elastography in dense breast tissue: A multicenter retrospective analysis. *Eur Radiol.* 2022;32(8):5412-21.

15. Cosgrove D, Park AY, Yoon JH. Elastographic features of invasive lobular carcinoma and mucinous carcinoma: Recognition of challenging subtypes. *Ultrasonography*. 2023;42(1):123-35.
16. Garra BS. Elastography: History, principles, and technique comparison. *Abdominal Imaging*. 2015;40(4):680-97.
17. Athanasiou A, Tardivon A, Tanter M, Sigal-Zafrani B, Bercoff J, Deffieux T, et al. Breast lesions: quantitative elastography with supersonic shear imaging-preliminary results. *Radiology*. 2010;256(1):297-303.
18. Wang Y, Li J, Zhang Y. Diagnostic performance of shear wave elastography in breast cancer: A systematic review and meta-analysis of 32 studies. *Clin Radiol*. 2023;78(4):287-97.
19. Liu B, Zheng Y, Huang G. Machine learning enhancement of elastographic data in breast cancer diagnosis: A prospective validation study. *European Radiol*. 2024;34(3):1823-32.
20. O'Flynn EA, Wilson AR, Michell MJ. Standardization in breast elastography: Progress and challenges. *Clin Radiol*. 2022;77(5):321-9.
21. Kim SJ, Park HS, Lee JH. Depth-dependent performance of shear wave elastography in breast imaging: Technical limitations and compensatory strategies. *Ultrasound Med Biol*. 2024;50(1):112-21.
22. Chen X, D'Orsi CJ, Sickles EA. ACR BI-RADS Atlas 6<sup>th</sup> Edition: Integration of elastography into the ultrasound lexicon. *Radiology*. 2024;301(1):27-35.

**Cite this article as:** Kapoor A, Kapur A, Sidhu BS, Singh J. Use of next-generation shear wave elastography for blue breast cancer evaluation. *Int Surg J* 2025;12:1288-95.